

## Effect of Skew and Radii Ratio on Motor Performance in Brushless Permanent Magnet Motors

Ali Jabbari<sup>+</sup>

Department of Mechanical Engineering, Qaemshahr Branch, Islamic Azad University, Qaemshahr, Iran

**Abstract.** In this paper, design optimization and fabrication of an interior permanent magnet motor is considered. A comparison of rotor iron pole radii and skew ratio effect on torque pulsation components is carried out using finite element analysis method and confirmed by experiment. The results show that, the skew method is very effective in suppressing the cogging torque of an interior permanent magnet motor. However, optimal radii ratio is more effective in torque ripple and reluctance torque reduction of pulsating torque components.

**Keywords:** design optimization, IPM motor, cogging torque, electromagnetic torque ripple, reluctance torque, radii ratio, skew ratio

### 1. Introduction

Interior permanent magnet (IPM) motors are suitable for industrial applications because of their high efficiency and compact configuration. Researchers have focused on design optimization of these motors to minimize pulsating torque components which may cause vibration and acoustic noises. Skewing is very effective in suppressing the cogging torque of an interior permanent magnet motor [1-8]. Recently, shape optimization is carried out to minimize these undesired effects. However, the effect of skewing and shape optimization on motor performance isn't compared so far.

In this paper, a comparison of rotor shape and skew ratio effect on pulsating torque components is carried out using FEA method and confirmed by experiment. The results show that, the skew method is very effective in suppressing the cogging torque of an interior permanent magnet motor. However, shape optimization is more effective in electromagnetic torque ripple and reluctance torque ripple reduction of pulsating torque components.

### 2. Design Specifications

A cross-section of the investigated motor which is a 3 phases, 8 poles-18 slots is shown in Fig.1 and characteristics of the motor which are the results of FEA method are listed in Table 1. Fig. 2 shows the FEA model of the motor.

Table 1 characteristics of the investigated motor

Parameter	Value
Pole number	8
Slot number	18
Phase number	3
PM flux density	1.17 T
Rotor outer diameter	33.5 mm
Magnet thickness	5 mm
Stator length	50 mm

<sup>+</sup> Corresponding author. Tel.: + (98-918-360-3558)  
E-mail address: ([jabbari84@gmail.com](mailto:jabbari84@gmail.com), [jabbari.ali@qaemshahriau.ac.ir](mailto:jabbari.ali@qaemshahriau.ac.ir)).

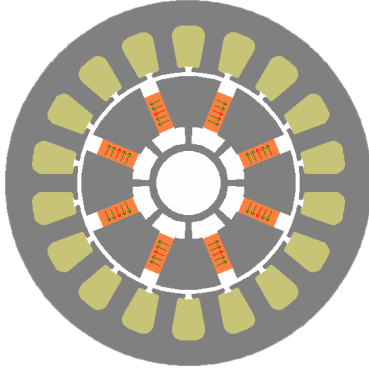


Fig. 1 Cross section of 8P18S IPM motor.

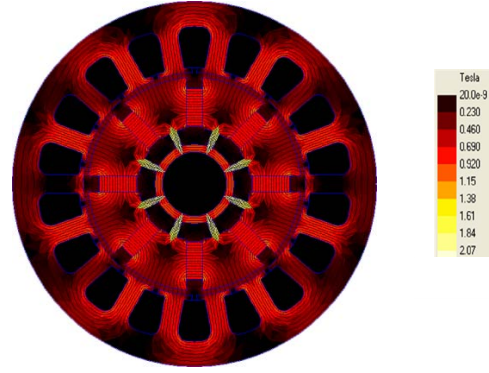


Fig. 2 FEA model of the IPM motor.

### 3. Design Optimization Variables

Design optimization is carried out using iron pole shape optimization and slot skewing method. In this section, radii ratio and skew ratio are defined as shape optimization and skewing variables, respectively.

Radii ratio is the ratio of rotor iron pole radius to maximum allowable radius of iron pole piece and is represented by  $\rho$ , i.e.

$$\rho = \frac{R}{R_{\max}} \quad (1)$$

The effect of radii ratio on motor pulsating torque components has been investigated by selecting 64 points with a step size of 0.5mm in interval of [11, 33.5] mm. Therefore, the  $\rho$  value is in interval of [0.328, 1].

The ratio of slot skew angle to slot pitch angle is defined as skew ratio and is represented by  $\alpha$ . Peak cogging torque curve versus skew ratio has four local minimum points for the investigated motor. The position of these points is consistent with the results of the following equation:

$$\alpha_{sk} = k \frac{N_s}{N_l} \quad (2)$$

Where,  $k = 1, 2, \dots, \frac{N_l}{N_s}$ . For the investigated motor,

$$\alpha_{sk} = k \frac{18}{18 \times 4} = \frac{k}{4} \quad (k = 1, 2, 3, 4)$$

Therefore the optimal  $\alpha_{sk}$  will be 0.25, 0.5, 0.75, and 1. Peak cogging torque shape is sine like. In  $\alpha=1$ , all harmonics of cogging torque will be cancelled.

## 4. Effect of Radii and Skew Ratio on Pulsating Torque Components

In this section, the effect of radii ratio and skew ratio on motor pulsating torque components has been studied.

### 4.1. Peak cogging torque comparison

By reducing the radii ratio ( $\rho$ ), peak cogging torque value (T-pk) decreases significantly from 0.01827N.m (at  $\rho=1$ ) to 0.0001003N.m (at  $\rho=0.343$ ) and then increases slightly to 0.0001668N.m (at  $\rho=0.328$ ), as shown in Fig. 3. In other words, a parabolic curve with a minimum at  $\rho=0.343$  can be adopted for cogging torque variations respect to radii. By reducing the radii, peak cogging torque variation rate decreases gradually from a sharp slope of 70.6° (at  $\rho=1$ ) to 0.126° (at  $\rho=0.343$ ).

By increasing skew ratio from zero to 0.25, peak value of cogging torque decreases with a sharp slope. From skew ratio of 0.25 to 0.375, peak value of cogging torque increases and then decreases to 0.5.

As shown in Fig. 4, after each minimal point, the position of peak and valley in the curve shifted by 2° mechanical degree, but the number of resting points is constant.

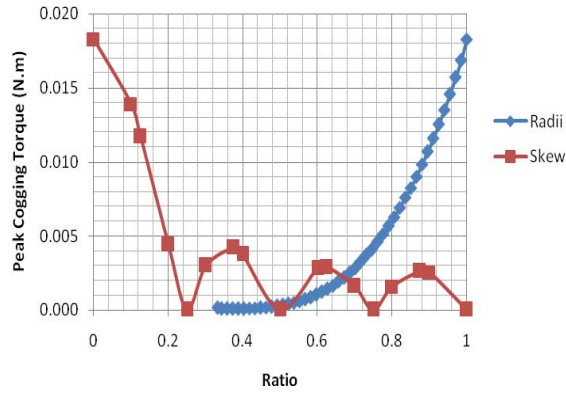


Fig.3 peak cogging torque variations respect to rotor iron pole radii.

### 4.2. Electromagnetic torque ripple comparison

As shown in Fig. 6, electromagnetic torque ripple decreases from 0.01139N.m (at  $\rho=0.582$ ) and then increases to 0.0205799N.m (at  $\rho=0.328$ ). Electromagnetic torque ripple decreases from 0.0761 (at  $\alpha=0$ ) to 0.0125999N.m (at  $\alpha=1$ ). The frequency of electromagnetic torque fluctuations decreases by reducing the radii. This means that the number of resting points per 180° electrical degree decreases.

### 4.3. Reluctance torque ripple

Average reluctance torque decreased to zero by reducing the radii, and then increases by further radii reduction, whereas, by increasing skew ratio, it will not decrease considerably. By reducing the radii, reluctance torque ripple decreases from 0.0170016N.m (at  $\rho=1$ ) to 0.000363207N.m (at  $\rho=0.477$ ) and then increases to 0.0051337N.m (at  $\rho=0.328$ ). By increasing skew ratio, it decreases from 0 to 0.25, increases from 0.25 to 0.375, decreases from 0.375 to 0.6, increases from 0.6 to 0.625, decreases from 0.625 to 0.75, increases from 0.75 to 0.875, decreases from 0.875 to 1. By increasing skew ratio, reluctance torque ripple will be decreased. Maximum value is 0.0761 N.m (at  $\alpha=0$ ) and minimal value is 0.0126N.m (at  $\alpha=1$ ).

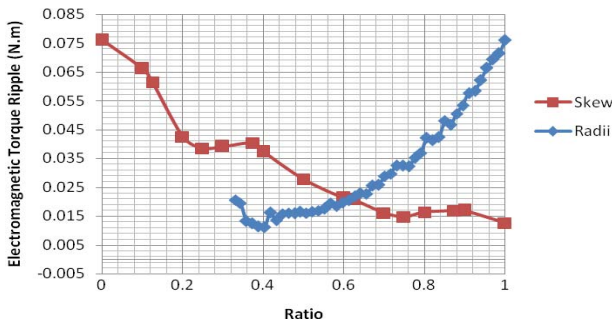


Fig. 5 Electromagnetic torque ripple versus skew ratio.

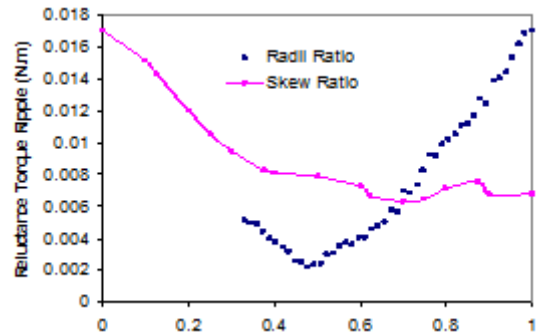


Fig. 6 Reluctance torque versus skew ratio.

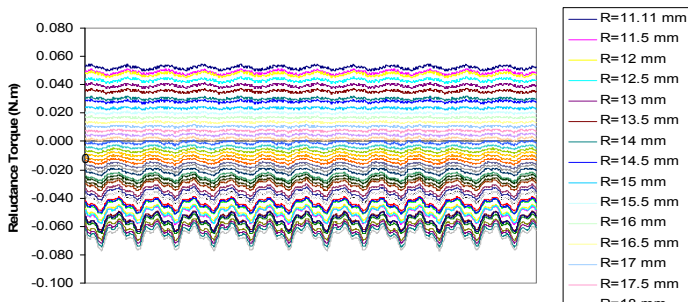


Fig. 7 Reluctance torque waveform versus radii.

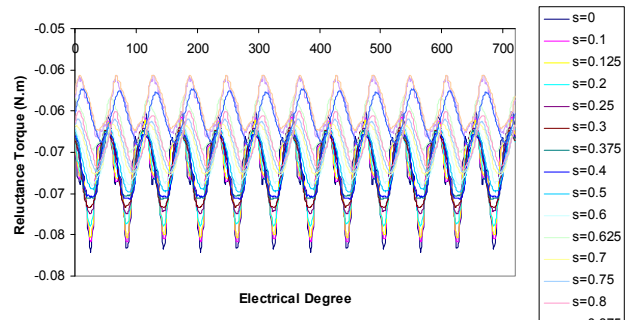


Fig. 8 Reluctance torque versus electrical degree

By reducing the radii, average value of reluctance torque reaches from -0.0085008N.m (at  $\rho=1$ ) to zero (at  $\rho=0.477$ ) and then to 0.00256685N.m (at  $\rho=0.328$ ).

Reluctance torque waveform is drawn for different skew ratios as shown in Fig. 8. A comparison with the effect of radii, average value of reluctance torque and its frequency does not change considerably. In other words, average value does not close to zero even at  $\alpha=1$ .

## 5. Experimental Investigation

The initial and optimal design of the investigated motor is shown in Fig. 9. The experimental results were obtained using the two laboratory prototypes fabricated based on initial and optimal design. As shown in Fig. 10, stator laminations have been fabricated using wire EDM process.

These laminations are assembled with permanent magnets on the rotor as shown in Fig.11. Based on the initial experimental set-up of the Fig. 11, a comparison of Back-EMF for initial and optimal design is derived. The results show that after optimization of radii, V-THD will be decreased 82% (from 9.12% at  $r=33.5\text{mm}$  to 1.64% at  $r=19.5\text{ mm}$ ) which is in good agreement with the FEM analysis result at optimum radii (82.1%).

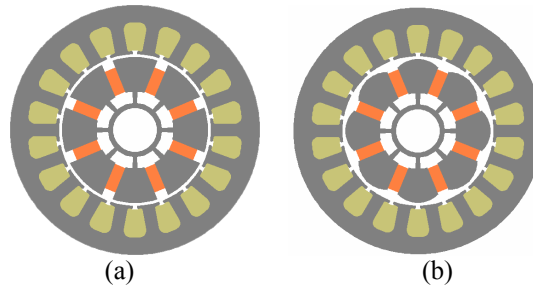


Fig. 9 Investigated motor, (a): initial, (b): optimized rotor.

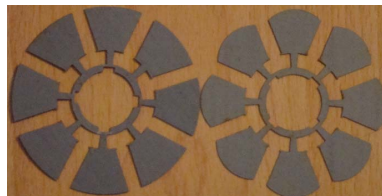


Fig. 10. laminations, Left: initial design, Right: optimal design.

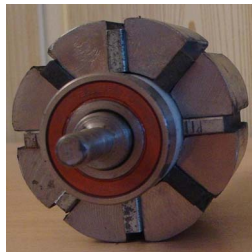


Fig. 12. The optimal rotor.



Fig. 13. Experimental set-up.

## 6. Conclusion

The effect of radii and skew ratio effect on motor performance is studied first by finite element analysis method and then is validated by experiment. Comparison results show that radii shape optimization is more effective than optimal skew ratios in reducing pulsating torque components.

## 7. References

- [1] Rajesh P. Deodhar, David A. Staton, Thomas M. Jahns, and J. E. Miller, "Prediction of Cogging Torque Using the Flux-MMF Diagram Technique" IEEE TRANSACTIONS ON INDUSTRY APPLICATIONS, VOL. 32, NO. 3, MAY/JUNE 1996.
- [2] G.H. Jang, J.W. Yoon, K.C. Ro, N.Y. Park and S.M. Jang, "Performance of a Brushless DC Motor due to the Axial Geometry of the Permanent Magnet," IEEE TRANSACTIONS ON MAGNETICS, VOL. 33, NO. 5, SEPTEMBER 1997.

- [3] D.C. Hanselman, "Effect of skew, pole count and slot count on brushless motor radial force, cogging torque and back EMF" IEE Proc-Electr. Power Appl., Vol. 144, No. 5. September 1997.
- [4] Min Dai, Ali Keyhani, and Tomy Sebastian, "Torque Ripple Analysis of a PM Brushless DC Motor Using Finite Element Method" IEEE TRANSACTIONS ON ENERGY CONVERSION, VOL. 19, NO. 1, MARCH 2004.
- [5] M. Łukaniszyn, M. JagieŁa, and R. Wróbel, "Optimization of Permanent Magnet Shape for Minimum Cogging Torque Using a Genetic Algorithm" IEEE TRANSACTIONS ON MAGNETICS, VOL. 40, NO. 2 MARCH 2004.
- [6] Mohammad S. Islam, Sayeed Mir, Tomy Sebastian, and Samuel Underwood, "Design Considerations of Sinusoidally Excited Permanent-Magnet Machines for Low-Torque-Ripple Applications" IEEE TRANSACTIONS ON INDUSTRY APPLICATIONS, VOL. 41, NO. 4, JULY/AUGUST 2005.
- [7] Delvis Anibal González, Juan Antonio Tapia, and Alvaro Letelier Bettancourt, "Design Consideration to Reduce Cogging Torque in Axial Flux Permanent-Magnet Machines" IEEE TRANSACTIONS ON MAGNETICS, VOL. 43, NO. 8, AUGUST 2007.
- [8] Li Zhu, S. Z. Jiang, Z. Q. Zhu, and C. C. Chan, "Analytical Methods for Minimizing Cogging Torque in Permanent-Magnet Machines" IEEE TRANSACTIONS ON MAGNETICS, VOL. 45, NO. 4, APRIL 2009.
- [9] E.R. Braga Filho and A.M.N. Lima, "Reducing Cogging Torque in Interior Permanent Magnet Machines without Skewing" IEEE TRANSACTIONS ON MAGNETICS, VOL 34, NO 5, SEPTEMBER 1998.
- [10] Dong-Hun Kim, Il-Han Park, Joon-Ho Lee, and Chang-Eob Kim, "Optimal Shape Design of Iron Core to Reduce Cogging Torque of IPM Motor" IEEE TRANSACTIONS ON MAGNETICS, VOL. 39, NO. 3, MAY 2003.
- [11] Joon-Ho Lee, Dong-Hun Kim, and Il-Han Park, "Minimization of Higher Back-EMF Harmonics in Permanent Magnet Motor Using Shape
- [12] Design Sensitivity With B-Spline Parameterization" IEEE TRANSACTIONS ON MAGNETICS, VOL. 39, NO. 3, MAY 2003.
- [13] Kyu-Yun Hwang, Sang-Bong Rhee, Byoung-Yull Yang, and Byung-Il Kwon, "Rotor Pole Design in Spoke-Type Brushless DC motor by Response Surface Method" IEEE TRANSACTIONS ON MAGNETICS, VOL. 43, NO. 4, APRIL 2007.
- [14] A. Kioumars, M. Moallem, and B. Fahimi, "Mitigation of Torque Ripple in Interior Permanent Magnet Motors by Optimal Shape Design" IEEE TRANSACTIONS ON MAGNETICS, VOL. 42, NO. 11, NOVEMBER 2006.
- [15] Y. Kawaguchi, T. Sato, I. Miki, and M. Nakamura, "A Reduction Method of Cogging Torque for IPMSM", 2007 IEEE.
- [16] Nicola Bianchi, Silverio Bolognani, Diego Bon, and Michele Dai Pr'e, "Rotor flux-barrier design for torque ripple reduction in synchronous reluctance motors" 2006 IEEE.
- [17] Sung-Il Kim, Ji-Young Lee, Young-Kyoun Kim, Jung-Pyo Hong, Yoon Hur, and Yeon-Hwan Jung, "Optimization for Reduction of Torque Ripple In Interior Permanent Magnet By Using the Taguchi Method" IEEE TRANSACTIONS ON MAGNETICS, VOL. 41, NO. 5, 2005.